East Eur. J. Phys. **3**. 49-54 (2021) DOI:10.26565/2312-4334-2021-3-07

PECULIARITIES IN THE STRUCTURE FORMATION AND CORROSION OF QUASICRYSTALLINE $Al_{65}Co_{20}Cu_{15}$ ALLOY IN NEUTRAL AND ACIDIC MEDIA[†]

Olena V. Sukhova*, Volodymyr A. Polonskyy
Oles Honchar Dnipro National University.
72, Haharin Ave., Dnipro, 49010, Ukraine
**Corresponding Author: sukhovaya@ukr.net*
Received June 23, 2021; revised August 16, 2021; accepted August 28, 2021

In the present study, the structure and corrosion properties of quasicrystalline conventionally solidified $Al_{65}Co_{20}Cu_{15}$ alloy cooled at 5 K/s were investigated. Structure was characterized by metallography, X-Ray diffraction, scanning electron microscopy, and energy dispersive spectroscopy. Corrosion properties were determined by gravimetric and potentiodynamic methods at room temperature. The investigations performed confirm the peritectic formation of stable quasicrystalline decagonal D-phase that coexists with crystalline $Al_4(Co,Cu)_3$ and $Al_3(Cu,Co)_2$ phases in the structure of $Al_{65}Co_{20}Cu_{15}$ alloy. According to energy dispersive spectroscopy, the stoichiometric composition of D-phase is $Al_{63}Co_{24}Cu_{13}$. The susceptibility of the $Al_{65}Co_{20}Cu_{15}$ alloy to corrosion significantly decreases with increasing pH from 1.0 (acidic media) to 7.0 (neutral medium). A corrosion rate of the $Al_{65}Co_{20}Cu_{15}$ alloy in the aqueous acidic solutions (pH=1.0) increases in the order $HNO_3 \rightarrow HCl \rightarrow H_2SO_4 \rightarrow H_3PO_4$. The mass of the specimens decreases in the solutions of H_2SO_4 or H_3PO_4 and increases in the solutions of HNO_3 or HCl which relates to different rate ratios of accumulation and dissolution of corrosion products. The $Al_{65}Co_{20}Cu_{15}$ alloy exhibits the highest corrosion resistance in the NaCl solution (pH=7.0) in which it corrodes under electrochemical mechanism with oxygen depolarization. The better corrosion resistance in sodium chloride solution is achieved due to the formation of passive chemical compounds blocking the surface. Free corrosion potential of the $Al_{65}Co_{20}Cu_{15}$ alloy has value –0.43 V, the electrochemical passivity region extends from –1.0 V to –0.4 V, and a corrosion current density amounts to 0.18 mA/cm^2. Depending on media, two typical surface morphologies are revealed after corrosion of quasicrystalline specimens of the $Al_{65}Co_{20}Cu_{15}$ alloy. In the H_2SO_4 and H_3PO_4 acidic solutions, clean specimens' surface due to its homogeneous dissolution is observed except for the more defective areas, such as boundaries of crystalline $Al_3(Cu,Co)_2$ phase containing less Co, which dissolve at a higher rate. In the HNO_3, HCl or NaCl solutions, a porous layer on the surface is formed which is visually revealed as surface darkening. After staying in the NaCl solution, on the surface of the $Al_{65}Co_{20}Cu_{15}$ alloy, the pits are also found due to preferential dissolution of components where the boundaries of $Al_3(Cu,Co)_2$ phase and flaws are located.
Keywords: quasicrystalline $Al_{65}Co_{20}Cu_{15}$ alloy, decagonal quasicrystals, structure, neutral and acidic aqueous solutions, corrosion resistance.
PACS: 61.50.Lt, 61.72.Ff, 62.23.Pq, 68.35 Fx, 68.35.Np, 81.05.Je, 81.40.Cd

The quasicrystalline alloys are considered to be particularly interesting metallic materials because of exceptional properties, or combinations of physical and chemical properties, that distinguish these alloys from conventional crystalline materials [1-5]. The quasicrystalline alloys are useful for industrial applications as engineering, structural and surface coating materials [6-17] due to their outstanding properties, including high strength and hardness, a low friction coefficient and excellent wear resistance, together with other remarkable engineering properties such as good oxidation resistance, high toughness etc. [18-26].

After the discovery of a metastable icosahedral quasicrystal in the Al–Mn system, many alloy systems have been identified in which icosahedral or decagonal quasicrystalline phases are stable up to melting temperature. Among them, the Al–Cu–Co system in which a stable decagonal phase (D-phase) has been found in a slowly solidified $Al_{65}Co_{20}Cu_{15}$ alloy [27-31]. D-phase is quasiperiodic in a plane and periodic in the ten-fold direction perpendicular to this plane [32-35]. From such crystal structure arises an attractive combination of certain properties that are not achievable with conventional crystalline alloys [36-39].

The presence of elements such as cobalt in the alloy composition may inhibit corrosion [40,41] and lead to greater corrosion resistance of quasicrystalline Al–Cu–Co alloys as compared with that of Al–Cu–Fe alloys that form icosahedral quasicrystalline phase [42-44]. But only limited information has been found in the literature concerning the susceptibility of the Al–Cu–Co alloys to corrosion. Therefore, in this study we explored the behaviour of the $Al_{65}Co_{20}Cu_{15}$ alloy in neutral and acidic media, which allows us to evaluate its corrosion resistance under conditions comparable to application of aviation and rocket-and-space equipment.

MATERIALS AND METHODS

The $Al_{65}Co_{20}Cu_{15}$ alloy was produced of high purity (99.99 %) components melted using Tamman furnace in a graphite crucible. The cooling rate of the alloy was 5 K/s. The alloy composition was verified by atomic absorption spectroscopy with Sprut CEΦ-01-M device. The relative precision of the measurements was better than ± 1 at. %.

Microstructural characterization of the investigated alloy was done using Neophot and GX-51 optical microscopes, Epiquant quantitative analyzer, JVC scanning electron microscope (SEM) equipped with energy-dispersive

[†] ***Cite as:*** O. V. Sukhova, and V. A. Polonskyy. East. Eur. J. Phys. **3**, 49 (2021), https://doi.org/10.26565/2312-4334-2021-3-07

spectrometer (EDS). The phase and structural compositions were also studied by powder X-ray diffraction (XRD) on ДРОН-УМ-1 diffractometer with Cu-K_α radiation.

The corrosion properties were investigated by the gravimetric method after holding the $Al_{65}Co_{20}Cu_{15}$ alloy for 1-4 h in the HCl, H_2SO_4, HNO_3, and H_3PO_4 aqueous acidic solutions (pH=1.0) and for 1–8 days in the NaCl aqueous neutral solution (pH=7.0). The pH value of the media was measured with an EB-74 ionometer. After immersion in solutions, the specimens were weighed in a BA-21 analytical balance with error smaller than 0.1 mg. A corrosion rate was determined using the equation given in [45].

Electrochemical experiments were conducted in the NaCl solution (pH=7.0) by means of ПІ-50-1 potentiostat and ПР-8 programmer using three-electrode electrolytic system consisted of the sample as working electrode, a platinum as counter electrode, and silver chloride as reference electrode. For each specimen, voltammograms were measured 2-3 times. A value of corrosion current density was determined by extrapolating the linear portion of the anodic and cathodic branches of the polarization curves to free corrosion potential. Model corrosion tests for 1–8 days in the NaCl solution were performed with specimens fully immersed in the medium. The surface morphology was examined using РЭМА 102-02 scanning electron microscope. Corrosion tests were carried out at the temperature of 293±2 K.

RESULTS AND DISCUSSION

Examination by optical and scanning electron microscopy reveals that $Al_{65}Co_{20}Cu_{15}$ alloy exhibits three-phase structure consisting of quasicrystalline decagonal D-phase and crystalline phases of $Al_4(Co,Cu)_3$ and $Al_3(Cu,Co)_2$ (Fig. 1a) [46]. The D-phase solidifies via a peritectic reaction, in which the primary $Al_4(Co,Cu)_3$ crystals are surrounded by the quasicrystalline phase. Later, liquid between D-quasicrystals solidifies to $Al_3(Cu,Co)_2$ phase. The identified phases are confirmed by X-ray investigation (Fig. 1b). EDS measurements show that D-phase has stochiometric composition $Al_{63}Co_{24}Cu_{13}$ (Table 1). This phase takes about 65 % of a total alloy volume. The size of quasicrystals varies from 40 to 60 μm due to differing local growth conditions.

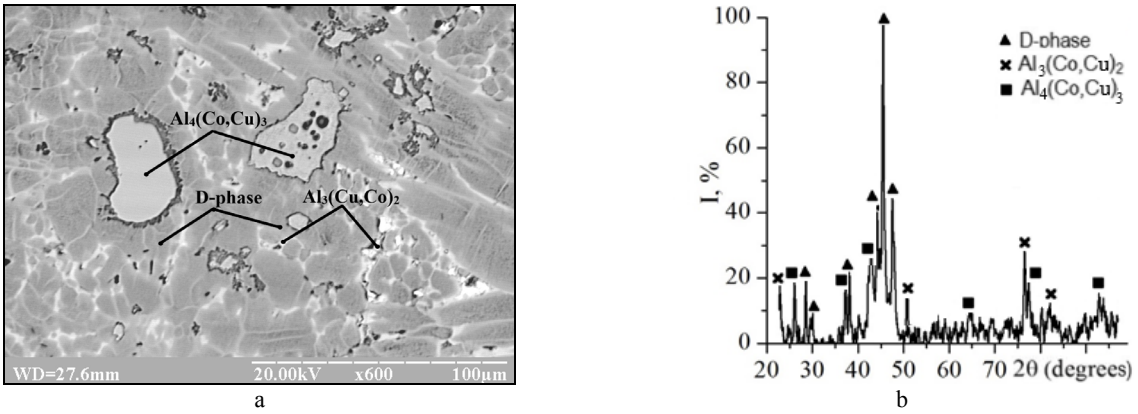

a b

Figure 1. The $Al_{65}Co_{20}Cu_{15}$ alloy: a – SEM image; b – XRD pattern

Table 1. Elemental analysis (in at. %) of the $Al_{65}Co_{20}Cu_{15}$ alloy

Phase	Al	Co	Cu
D-phase	62.99	24.02	12.99
$Al_4(Co,Cu)_3$	56.39	33.86	9.75
$Al_3(Cu,Co)_2$	59.48	9.71	30.81

Corrosion tests of the $Al_{65}Co_{20}Cu_{15}$ alloy in the acidic media show that after the first hour of treatment a mass of the specimens gradually increases in the nitric and chloric acids. The mass gain in the chloric acid significantly exceeds that in the nitric acid reaching 4.58 g/m^2 against 0.98 g/m^2 after 4 holding hours. At that, the biggest relative change in the mass is observed after 2 holding hours in the chloric acid and after 3 holding hours in the nitric acid (Table 2).

Table 2. Relative changes in the mass (in %) of specimens of the $Al_{65}Co_{20}Cu_{15}$ alloy after corrosion tests

Solution	Holding time, hours				
	1	2	3	4	
HCl	0.02	0.04	0.12	0.14	
HNO_3	0.00	0.00	0.01	0.03	
H_2SO_4	-0.01	-0.09	-0.15	-0.18	
H_3PO_4	-0.02	-0.09	-0.23	-0.25	
NaCl	Holding time, days				
	1	2	3	4	8
	0.04	0.15	0.20	0.22	0.24

After staying in the H_2SO_4 and H_3PO_4 acidic solutions, the mass of the specimens, on the contrary, decreases, and after 4 holding hours specific changes of the mass equal to –5.89 g/m^2 and –8.18 g/m^2 correspondingly. The $Al_{65}Co_{20}Cu_{15}$ alloy turns out to be the most corrosion-sensitive in the H_3PO_4 acid. The samples mainly lose their mass in the sulphuric acidic solution after 1 holding hour and in the orthophosphate acidic solution after 2 holding hours (Table 2). This conclusion is confirmed by scanning electron microscopy of the surface of the $Al_{65}Co_{20}Cu_{15}$ alloy affected by the sulphuric acidic solution (Fig. 2). The surface of the specimens quite homogeneously dissolves where Co-rich quasicrystalline D-phase and crystalline $Al_4(Co,Cu)_3$ phase are located (Fig. 2b). Whereas, crystalline $Al_3(Cu,Co)_2$ phase, containing less Co, dissolves at a higher rate which may relate also to the fact that this phase crystallizes last and, therefore, may have more defective structure (Fig. 2a).

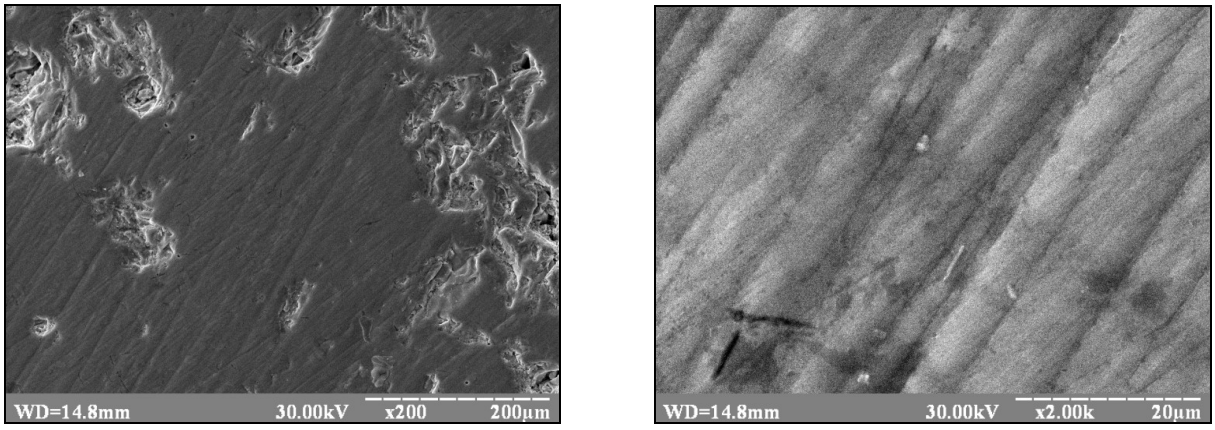

a b

Figure 2. SEM-images of surface of the $Al_{65}Co_{20}Cu_{15}$ alloy after 4 holding hours in sulphuric acidic solution (pH=1.0)

The revealed differences in the mass changes of the corroded $Al_{65}Co_{20}Cu_{15}$ alloy affected by the acids may be explained by different rate ratios of selective dissolution of the alloy components and accumulation of corrosion products on the specimens` surface. Comparison of corrosion rates of the alloy for the investigated acidic solutions exhibits the following sequence $HNO_3 \rightarrow HCl \rightarrow H_2SO_4 \rightarrow H_3PO_4$ (in ascending order) (Fig. 3).

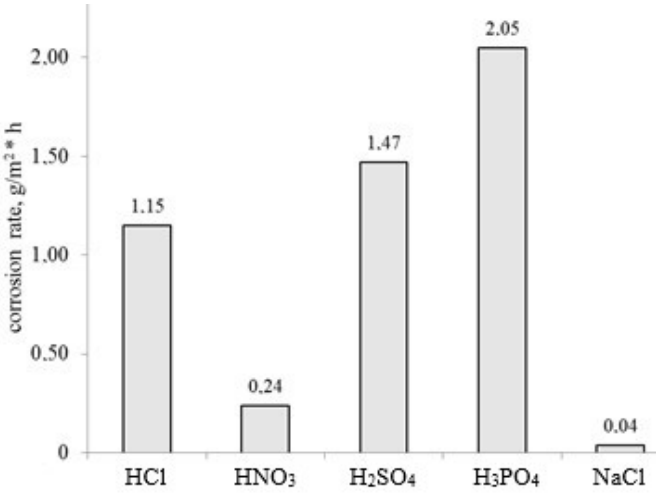

Figure 3. Corrosion rates of the $Al_{65}Co_{20}Cu_{15}$ alloy in the investigated corrosion media

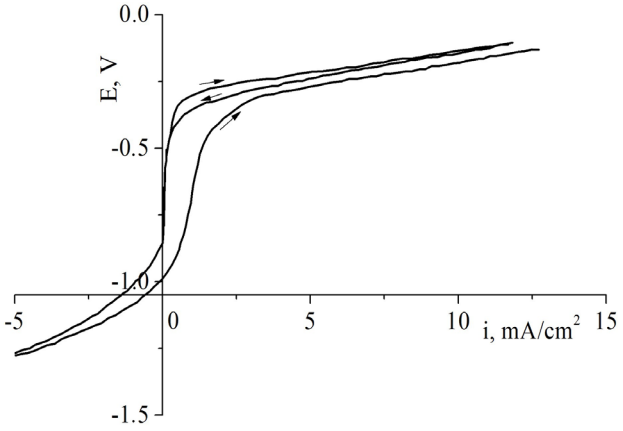

Figure 4. Potential versus current curves of the corrosion in NaCl solution (pH=7) of the $Al_{65}Co_{20}Cu_{15}$ alloy

When subjected to corrosion in the investigated media, the analyzed $Al_{65}Co_{20}Cu_{15}$ alloy is found to corrode much weaker in the NaCl solution (pH=7.0) than in the acidic solutions of HNO_3, H_2SO_4, HCl, and H_3PO_4 (pH=1.0). After 8 days of the tests in the aqueous sodium chloride solution, the specific mass change of the $Al_{65}Co_{20}Cu_{15}$ alloy equals to 8.0 g/m^2. On the surface of the samples, a passivating oxide film is formed during the tests, which is revealed visually as surface darkening. That is why, the results on changes in the mass of specimens relative to the initial value indicate that the mass of specimens gradually increases, especially after 1 day of treatment (Table 2). Then, after 3 days of staying in the NaCl solution, the mass of specimens increases to a much lesser extent.

Chronopotentiometry measurements of free corrosion potential of the $Al_{65}Co_{20}Cu_{15}$ alloy show that potential stabilizes at a value of –0.43 V after ~17 minutes of measurements. A steady potential testifies that the passivation film build-up in the NaCl solution remains protective. Polarization measurements also evidence that corrosion of the $Al_{65}Co_{20}Cu_{15}$ alloy in the sodium chloride solution is typical to processes with oxygen depolarization (Fig. 4). Voltammograms recorded in semi-logarithmic coordinates indicate that anodic current gradually increases as potential changes towards more positive values. A sharp increase of an anodic current is observed at potential of ~–0.3 V due to beginning of active dissolution of the alloy components. The appearance of a hysteresis loop in the anodic regime may be attributed to the surface passivation. After changing the direction of a potential sweep, in the cathodic area of a plot, a current limit in the mA range is observed. The zero value of a current density is reached at potential of –0.87 V. At potentials more negative than –1.0 V, cathodic current increases which relates to active hydrogen evolution. The value of corrosion current density for the alloy is 0.18 mA/cm^2. The electrochemical passivity region extends from –1.0 V to –0.4 V which indicates that the $Al_{65}Co_{20}Cu_{15}$ alloy is not susceptible to corrosion in the NaCl solution due to inhibition of anodic processes. That is why, the $Al_{65}Co_{20}Cu_{15}$ alloy exhibits the lowest corrosion rate at higher pH (Fig. 3).

Scanning electron microscopic investigations evidence that on the corroded surface of the $Al_{65}Co_{20}Cu_{15}$ alloy after staying in the NaCl solution for 8 days, pits about 10 μm in size are observed located mainly in the vicinity of defects (Fig. 5a). Corrosion is mainly concentrated in crystalline $Al_3(Cu,Co)_2$ phase containing less Co. The dissolution of this phase is most intense near the phase boundaries (Fig. 5b). Meanwhile, Co-rich quasicrystalline D-phase and crystalline $Al_4(Co,Cu)_3$ phase are less susceptible to corrosion.

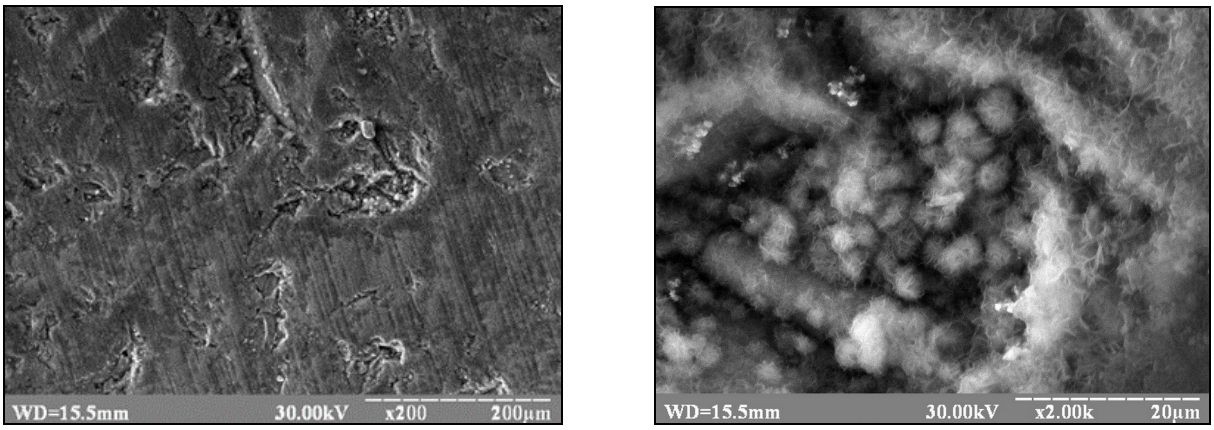

a b

Figure 5. SEM-images of surface of the $Al_{65}Co_{20}Cu_{15}$ alloy after holding for 8 days in the NaCl solution (pH=7.0)

CONCLUSIONS

The investigations made on conventionally solidified $Al_{65}Co_{20}Cu_{15}$ alloy confirm that alloy system cooled at 5 K/s forms stable quasicrystalline decagonal D-phase by peritectic reaction. Its stoichiometric composition corresponds to $Al_{63}Co_{24}Cu_{13}$.

Corrosion of the $Al_{65}Co_{20}Cu_{15}$ alloy in the acidic solutions (pH=1.0) of HNO_3, HCl, H_2SO_4, H_3PO_4 (in ascending order) is much stronger than in the NaCl neutral solution (pH=7.0), intensifying with pH decreasing. The corrosion rate is lower by a factor between 6.0 and 51.25 as pH value is raised from 1.0 to 7.0. In the aqueous solutions of HNO_3, HCl, and NaCl, a rate of accumulation of corrosion products on the specimens' surface exceeds a rate of dissolution of alloy components, but in the solutions of H_2SO_4 and H_3PO_4 – vice versa. The surface of the specimens is dissolved almost homogeneously except for the boundaries of crystalline $Al_3(Cu,Co)_2$ phase containing less Co which dissolve at a higher rate.

The corrosion of the $Al_{65}Co_{20}Cu_{15}$ alloy in the NaCl aqueous solution (pH=7.0) proceeds by the electrochemical mechanism with oxygen depolarization. The highest corrosion resistance of the $Al_{65}Co_{20}Cu_{15}$ alloy is observed in neutral media where a protective oxide film is developed. This alloy has free corrosion potential –0.43 V, electrochemical passivity region extending from –1.0 V to –0.4 V, and the value of corrosion current density – 0.18 mA/cm^2. On the surface affected by saline solution, the pits are revealed preferentially where the phase boundaries and flaws are located.

The work was performed within the framework of research project No. 0119U100977 "Electrode reactions of 3d-metal π-complexes" (2019-2021).

ORCID IDs

Olena V. Sukhova, https://orcid.org/0000-0001-8002-0906; **Volodymyr A. Polonskyy,** https://orcid.org/0000-0002-4810-2626

REFERENCES

[1] C. Janot, *Quasicrystals*, (Springer, Berlin, Heidelberg, 1994), https://doi.org/10.1007/978-3-662-22223-2_9.
[2] Z.M. Stadnik, *Physical Properties of Quasicrystals*, (Springer-Verlag, Berlin Heidelberg, 1999), https://doi.org/10.1007/978-3-642-58434-3.
[3] H.R. Trebin, *Quasicrystals: Structure and Physical Properties*, (Wiley-VCH Verlag GmbH & Co., Weinheim, 2003), https://doi.org/10.1002/3527606572.
[4] J.-M. Dubois, Chem. Soc. Rev. **41**, 4760-4777 (2012), https://doi.org/10.1039/C2CS35110B.
[5] E. Huttunen-Saarivirta, J. Alloys Compd. **363**(1-2), 150-174 (2004), https://doi.org/10.1016/S0925-8388(0)00445-6.
[6] I.M. Spyrydonova, O.V. Sukhova, and G.V. Zinkovskij, Metall. Min. Ind. **4**(4), 2-5 (2012). (in Russian)
[7] W. Wolf, C. Bolfarini, C.S. Kiminami, and W.J. Botta, J. Mater. Res. **36**, 281-297 (2021), https://doi.org/10.1557/s43578-020-00083-4.
[8] K. Jithesh, T.R. Prabhu, R.V. Anant, M. Arivarasu, A. Srinivasan, R.K. Mishra, and N. Arivazhagan, Mater. Sci. Forum. **969**, 218-224 (2019), https://doi.org/10.4028/www.scientific. net/MSF.969.218.
[9] I.M. Spiridonova, E.V. Sukhovaya, S.B. Pilyaeva, and O.G. Bezrukavaya, Metall. Min. Ind. **3**, 58-61 (2002). (in Russian)
[10] M. Kamalnath, B. Mohan, A. Singh, and K. Thirumavalavan, Mater. Res. Express. **7**(2), 1-11 (2020), https://doi.org/10.1088/2053-1591/ab71c5.
[11] O.V. Sukhova, Phys. Chem. Solid St. **21**(2), 355-360 (2020), https://doi.org/10.15330/pcss.21.2.355-360.
[12] M. Zhu, G. Yang, L. Yao, S. Cheng, and Y. Zhou, J. Mater. Sci. **45**(14), 3727-3734 (2010), https://doi.org/10.1007/s10853-010-4421-8.
[13] O.V. Sukhova and Yu.V. Syrovatko, Metallofiz. Noveishie Technol. **33**(Special Issue), 371-378 (2011). (in Russian)
[14] V.V. Cherdyntsev, S.D. Kaloshkin, I.A. Tomilin, E.V. Shelekhov, A.I. Laptev, A.A. Stepashkin, and V.D. Danilov, Phys. Met. Metallogr. **104**(5), 497-504 (2007), https://doi.org/10.1134/S0031918X0711009.
[15] T.P. Yadav, D. Singh, R.S. Tiwari, and O.N. Srivastava, J. Mater. Lett. **80**, 5-8 (2012), https://doi.org/10.1016/ J.MATLET.2012.04.034.
[16] S.I. Ryabtsev, V.A. Polonskyy, and O.V. Sukhova, Powder Metall. Met. Ceram. **58**(9-10), 567-575 (2020), https://doi.org/10.1007/s11106-020-00111-2.
[17] J. Krawczyk, W. Gurdziel, W. Bogdanowicz, and K. Flisinski, Solid State Phenom. **163**, 282-285 (2010), https://doi.org/ 10.4028/ www.scientific.net/SSP.163.282.
[18] O.V. Sukhova and K.V. Ustinova, Funct. Mater. **26**(3), 495-506 (2019), https://doi.org/10.15407/fm26.03.495.
[19] S.S. Kang and J.-M. Dubois, Phil. Mag. A. **66**(1), 151-163 (1992), https://doi.org/10.1080/01418619208201520.
[20] U. Koster, W. Liu, H. Liebertz, and M. Michel, J. Non-Cryst. Solids. **153-154**, 446-452 (1993), https://doi.org/10.1016/0022-3093(93)90393-C.
[21] X. Zhou, P. Li, J. Luo, S. Qian, and J. Tong, J. Mater. Sci. Technol. **20**(6), 709-713 (2009), https://jmst.org/CN/Y2004/V20/106/709.
[22] B.I. Wehner, J. Meinhardt, U. Koster, H. Alves, N. Eliaz, and D. Eliezer, Mater. Sci. Eng. A. **226-228**, 1008-1011 (1997), https://doi.org/10.1016/S0921-5093(96)10848-0.
[23] L.C. Jamshidi and R.J. Bodbari, J. Chilean Chem. Soc. **63**(2), 3928-3933 (2018), https://doi.org/10.4067/s0717-97072018000203928.
[24] L.C. Jamshidi, R.J. Rodbari, L. Nascimento, E.P. Hernandez, and C.M. Barbosa, J. Met. Mater. Miner. **26**(1), 9-16 (2016), https://doi.org/10.14456/jmmm.2016.2.
[25] K. Yubuta, K. Yamamoto, A. Yasuhara, and K. Hiraga, Mater. Trans. **55**(6), 866-870 (2014), https://doi.org/10.2320/matertrans.M2014008.
[26] R.A. Varin, L. Zbroniec, T. Czujko, and Y.-K. Song, Mater. Sci. Eng. A. **300**(1-2), 1-11 (2001), https://doi.org/10.1016/S0921-5093(00)01809-8.
[27] A.-P. Tsai, A. Inoue, and T. Masumoto, Mater. Trans. JIM. **30**(4), 300-304 (1989), https://doi.org/10.2320/matertrans1989.30.300.
[28] I.M. Zhang and P. Gille, J. Alloys Compd. **370**(1-2), 198-205 (2004), https://doi.org/10.1016/j.jallcom.2003.09.033.
[29] D. Holland-Moritz, D.M. Herlach, B. Grushko, and K. Urban, Mater. Sci. Eng. A. **181-182**, 766-770 (1994), https://doi.org/10.1016/0921-5093(94)90735-8.
[30] W. Bogdanowicz and J. Krawczyk, Cryst. Res. Technol. **45**(12), 1321-1325 (2010), https://doi.org/10.1002/crat.201000313.
[31] D. Holland-Moritz, G. Jacobs, and I. Egry, Mater. Sci. Eng. **294-296**, 369-372 (2000), https://doi.org/10.1016/S0921-5093(00)01126-6.
[32] Y. Zou, P. Kuczera, J. Wolny, Acta Phys. Pol. A. **130**(4), 845-847 (2016), https://doi.org/10.12693/aphyspola.130.845.
[33] B. Luca, J. Pham, and P.J. Steinhardt, Sci. Rep. 8, 1-8 (2018), https://doi.org/10.1038/s41598-018-34375-x.
[34] M. Widom, I. Al-Lehyani, W. Wang, and E. Cockayne, Mater. Sci. Eng. **294-296**, 295-298 (2000), https://doi.org/10.1016/S0921-5093(00)01215-6.
[35] E. Cockayne and M. Widom, Phys. Rev. Lett. **81**(3), 598-601 (1998), https://doi.org/10.1103/PhysRevLett.81.598.
[36] A.R. Kortan, F.A. Thiel, H.S. Chen, A.P. Tsai, A. Inoue, and T. Masumoto, Phys. Rev. B. **40**(13), 9397-9399 (1989), https://doi.org/10.1103/PhysRevB.40.9397.
[37] D. Holland-Moritz, J. Schroers, D.M. Herlach, B. Grushko, and K. Urban, Acta Mater. **46**(5), 1601-1615 (1998), https://doi.org/10.1016/S1359-6454(97)00341-8.
[38] X.Z. Liao, X.L. Ma, J.Z. Jin, and K.H. Kuo, J. Mater. Sci. Lett. 11, 909-912 (1992), https://doi.org/10.1007/BF00729091.
[39] L. Bindi, N. Yao, C. Lin, L.S. Hollister, C.L. Andronicos, V.V. Distler, M.P. Eddy, A. Kostin, V. Kryachko, G.J. MacPherson, W.M. Steinhard, M.P. Yudovskaya, and L. Steinhard, Sci. Rep. 5, 1-5 (2015), https://doi.org/10.1038/srep09111.
[40] K. Cooke, *Aluminum Alloys and Composites*, (Intechopen, London, 2020), https://doi.org/10.5772/intechopen.81519.
[41] I.M. Spiridonova, E.V. Sukhovaya, V.F. Butenko, A.P. Zhudra, A.I. Litvinenko, and A.I. Belyi, Powder Metall. Met. Ceram. **32**(2), 139-141 (1993), https://doi.org/10.1007/BF00560039.
[42] O.V. Sukhova, V.A. Polonskyy, and K.V. Ustinova, Metallofiz. Noveishie Technol. **40**(11), 1475-1487 (2018), https://doi.org/10.15407/mfint.40.11.1475. (in Ukrainian)
[43] O.V. Sukhova, V.A. Polonskyy, and K.V. Ustinova, Voprosy Khimii i Khimicheskoi Technologii. **6**(121), 77-83 (2018), https://doi.org/10.32434/0321-4095-2018-121-6-77-83. (in Ukrainian)

[44] O.V. Sukhova, V.A. Polonskyy, and K.V. Ustinova, Phys. Chem. Solid St. **18**(2), 222-227 (2017), https://doi.org/10.15330/pcss.18.2.222-227.
[45] I.M. Zharskyy, N.P. Ivanova, D.V. Kuis, and N.A. Svidunovich, *Коррозия и защита металлических конструкций и оборудования* [*Corrosion and Protection of Metal Constructions and Equipment*], (Vysh. shk., Minsk, 2012). (in Russian)
[46] O.V. Sukhova and Yu.V. Syrovatko, Metallofiz. Noveishie Technol. **41**(9), 1171-1185 (2019), https://doi.org/10.15407/mfint.41.09.1171. (in Russian)

ОСОБЛИВОСТІ СТРУКТУРОУТВОРЕННЯ ТА КОРОЗІЇ КВАЗІКРИСТАЛІЧНОГО СПЛАВУ $Al_{65}Co_{20}Cu_{15}$ В НЕЙТРАЛЬНОМУ ТА КИСЛИХ СЕРЕДОВИЩАХ

Олена В. Сухова, Володимир А. Полонський
Дніпровський національний університет імені Олеся Гончара
49010, Україна, м. Дніпро, просп. Гагаріна, 72

В роботі досліджували структуру та корозійні властивості квазікристалічного сплаву $Al_{65}Co_{20}Cu_{15}$, закристалізованого зі швидкістю 5 К/с за звичайних умов. Структуру вивчали методами металографії, рентгеноструктурного аналізу, сканувальної електронної мікроскопії та рентгеноспектрального мікроаналізу. Корозійні властивості визначали гравіметричним та потенціодинамічним методами за кімнатної температури. Проведені дослідження підтвердили перитектичне утворення стабільної квазікристалічної декагональної D-фази, яка в структурі сплаву $Al_{65}Co_{20}Cu_{15}$ співіснує з кристалічними фазами $Al_4(Co,Cu)_3$ та $Al_3(Cu,Co)_2$. Згідно з результатами рентгеноспектрального мікроаналізу, стехіометричний склад D-фази відповідає $Al_{63}Co_{24}Cu_{13}$. Опір корозії сплаву $Al_{65}Co_{20}Cu_{15}$ суттєво збільшується з підвищенням pH розчинів з 1,0 (кислі середовища) до 7,0 (нейтральне середовище). Швидкість корозії сплаву $Al_{65}Co_{20}Cu_{15}$ у водних розчинах кислот (pH=1,0) збільшується в такому порядку: $HNO_3 \rightarrow HCl \rightarrow H_2SO_4 \rightarrow H_3PO_4$. Маса зразків зменшується в розчинах кислот H_2SO_4 та H_3PO_4 і збільшується в розчинах HNO_3 та HCl, що пов'язане з різним співвідношенням швидкостей накопичення та розчинення продуктів корозії. Найбільшу корозійну тривкість сплав $Al_{65}Co_{20}Cu_{15}$ має в розчині NaCl (pH=7,0), в якому корозія сплаву проходить за електрохімічним механізмом з кисневою деполяризацією. Найкращий опір корозії в розчині натрій хлориду досягається за рахунок утворення пасивних хімічних сполук на поверхні сплаву, які блокують корозію. Вільний потенціал корозії сплаву $Al_{65}Co_{20}Cu_{15}$ становить –0,43 В, зона електрохімічної пасивності простягається від –1,0 В до –0,4 В, а густина струму корозії дорівнює 0,18 мА/см^2. Залежно від корозійного середовища, спостерігаються два типи поверхні зразків квазікристалічного сплаву $Al_{65}Co_{20}Cu_{15}$, які зазнали корозійного руйнування. Після перебування в розчинах кислот H_2SO_4 та H_3PO_4 спостерігається чиста поверхня зразків внаслідок її відносно рівномірного розчинення за виключенням більш дефектних ділянок, таких як границі кристалічної фази $Al_3(Cu,Co)_2$, що містить менше Co, які розчиняються дещо швидше. В розчинах HNO_3, HCl та NaCl на поверхні утворюється пористий шар, який візуально спостерігається як потемніння поверхні. Після перебування в розчині NaCl на поверхні сплаву $Al_{65}Co_{20}Cu_{15}$ також утворюються ділянки пітінгів внаслідок переважного розчинення компонентів в місцях розташування границь фази $Al_3(Cu,Co)_2$ та дефектів поверхні.

Ключові слова: квазікристалічний сплав $Al_{65}Co_{20}Cu_{15}$, декагональні квазікристали, структура, нейтральний та кислі водні розчини, корозійна тривкість.